INVESTIGATION OF HIGH-EFFICIENCY SCREEN-PRINTED TEXTURED SI SOLAR CELLS WITH HIGH SHEET-RESISTANCE EMITTERS

Mohamed M. Hilali, Kenta Nakayashiki, Abasifreke Ebong and Ajeet Rohatgi
University Center of Excellence for Photovoltaics Research and Education,
School of Electrical and Computer Engineering, Georgia Institute of Technology, Atlanta, GA 30332-0250

ABSTRACT

In this study it is found that the efficiency enhancement ($\Delta\eta$) resulting from the use of a 100 Ω/sq emitter instead of a conventional 45 Ω/sq emitter is substantially enhanced further by surface texturing. This enhancement is greater for textured cells by at least ~0.4% absolute over the enhancement for planar cells, and is mainly due to the greater difference in the front-surface recombination velocity (FSRV) between the high- and low-sheet-resistance emitter textured cells. A FSRV of 60,000 cm/s resulted in a reasonably good V_{oc} of ~642 mV for the 100 Ω/sq emitter textured cell. Our investigation of the Ag-Si contact interface shows a more regular distribution of Ag crystallite precipitation for the textured emitter (mainly at the peaks of the texture pyramids). The high contact-quality resulted in a series resistance of 0.79 Ω-cm, a junction leakage current of 18.5 nA/cm^2 yielding a FF of 0.784. This resulted in a record high-efficiency 4 cm^2 screen-printed cell of 18.8% (confirmed by NREL) on textured 0.6 Ω-cm FZ, with single-layer antireflection coating.

INTRODUCTION

The cost performance targets of Si photovoltaics can be reached by enhancing cell efficiency while utilizing high throughput processing [1]. Front-surface texturing and high sheet-resistance emitters have consistently enhanced the solar cell performance resulting in high efficiencies [2-4]. However, they have not yet been implemented together using the simple conventional screen-printed cell processing (i.e. single-step diffusion and co-firing of the screen-printed contacts). Therefore, in this study, we have investigated the combination of high sheet-resistance emitters with surface texturing using screen-printed contacts. We have previously demonstrated high fill factors (>0.78) on high sheet-resistance planar emitters through understanding and optimization of an appropriate Ag paste and firing recipe [5]. This led to the fabrication of 17.4%-efficient solar cells on float-zone Si with screen-printed contacts on a planar 100 Ω/sq phosphorus-doped emitter. In this paper we report on the investigation of textured high sheet-resistance emitters. Both the short-wavelength response and the screen-printed contact behavior for high sheet-resistance emitter textured cells have been investigated. A study of these factors has been also performed for planar cells.

EXPERIMENTAL

In this study, screen-printed (SP) n^+-p-p^+ solar cells (4 cm^2) are fabricated on single-crystal p-type, 300-μm thick (100) float-zone (FZ) substrates. First, textured and planar FZ silicon wafers received a standard RCA clean followed by $POCl_3$ diffusion to form the n^+-emitter. A diffusion temperature of 843°C was used for the 100 Ω/sq emitter while 878°C was used for the 45 Ω/sq. After the phosphorus-glass removal and another clean, 50 kHz PECVD SiN_x AR coating was deposited on the emitter. Next, an Al paste was screen-printed on the backside and dried at 200°C. The Ag grid was then screen-printed on top of the SiN_x film and then the Ag and Al contacts were co-fired (single firing step) in a lamp-heated three-zone infra-red belt furnace. Cells were then isolated using a dicing saw and then subjected to a 15-min. forming-gas anneal. The cell performance was characterized by light I-V as well as internal quantum-efficiency (IQE) measurements for the short-wavelength response. Textured cells were used with planar back to ensure that the base properties were the same when comparing planar and textured cells. Cells with surface texturing on both sides were also fabricated.

RESULTS AND DISCUSSION

As shown in Fig. 1 the short-wavelength response for a textured emitter is lower than that for the planar emitter. This is attributed to the higher front-surface recombination velocity because of the increase in surface area due to the textured surface. Nevertheless, the lower reflectance due to texturing results in a 3.94 mA/cm^2 enhancement in transmitted current over the planar surface, calculated from the reflectance curves in Fig. 2. Therefore, the loss in short-wavelength response shown in Fig. 1 is relatively negligible.

As shown in Fig. 3, the enhancement in efficiency due to the 100 Ω/sq emitter compared with a 45 Ω/sq emitter is significantly more pronounced for textured cells

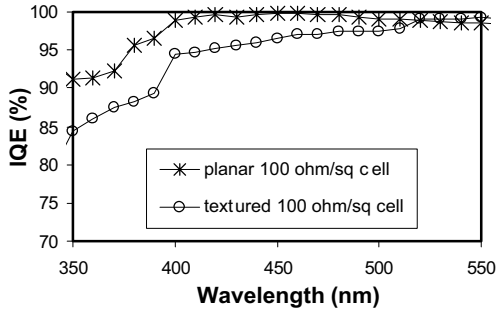

Fig. 1: Short-wavelength response of planar versus textured 100 Ω/sq emitters.

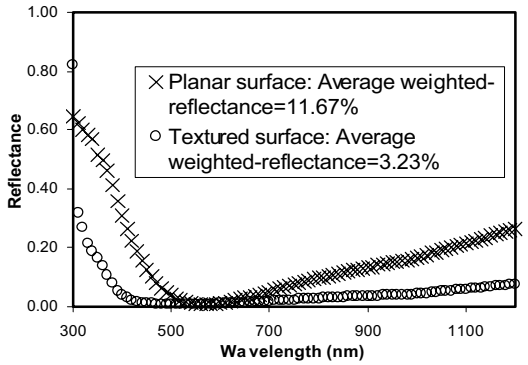

Fig. 2: Reflectance of planar and textured emitter surface with SiN_x single-layer antireflection coating.

compared with planar cells. The higher $\Delta\eta$ shown in Fig. 3 for textured cells is a result of a higher ΔJsc by ~0.4 mA/cm^2 for the textured cells compared with the planar cells (Table 1). The improvement in J_{sc} (ΔJ_{sc}) due to the 100 Ω/sq over a 45 Ω/sq emitter for textured cells is ~1.2 mA/cm^2 while that for planar cells is ~0.8 mA/cm^2 for the 0.6 Ω-cm base resistivity. The V_{oc} enhancement for textured cells is the same as for the planar cells, and the fill factors are within close range for the textured and planar cells with the same emitter sheet-resistance. Therefore, we investigated the IQE as well as the spectral response (SR) for the 45 and 100 Ω/sq textured and planar cells to better understand the difference in ΔJ_{sc} between planar and textured cells. SR is expressed as: $SR(\lambda)=IQE(\lambda)(1-R(\lambda))\cdot(\lambda/1.24)$,
where IQE is the internal quantum efficiency, R is the reflectance of the cell, and λ is the wavelength in μm.

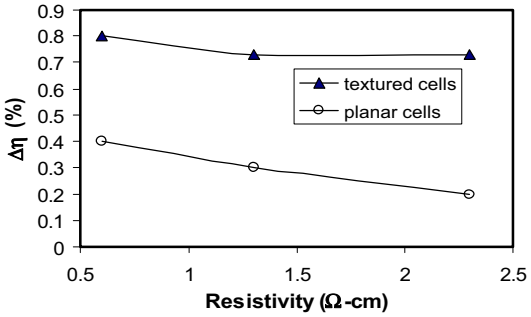

Fig. 3: Measured enhancement in efficiency due to a 100 Ω/sq versus a 45 Ω/sq emitter for textured and planar cells with different base resistivity.

Table 1: Light I-V parameters of 0.6 Ω-cm textured and planar best cells with 45 and 100 Ω/sq emitters.

Emitter Surface	Emitter (Ω/sq)	V_{oc} (mV)	J_{sc} (mA/cm^2)	ΔJsc (mA/cm^2)	FF	Eff (%)	Δη (%)
Planar	45	636	33.8	0.8	0.786	17.0	0.4
	100	646	34.6		0.780	17.4	
Textured	45	632	35.7	1.2	0.781	17.6	0.8
	100	642	36.9		0.778	18.4	

A. Investigation of the Short-Wavelength Response

There are three possibilities for the greater enhancement in J_{sc} for the textured high sheet-resistance emitter compared with the low sheet-resistance emitter. The first factor investigated is the enhancement in IQE (ΔIQE, the enhancement in IQE due to the high sheet-resistance emitter) due to the longer light path for a textured emitter versus a planar emitter. The increased light path increases absorption for a textured surface since the absorption for a textured surface is $\alpha_{tex}=\alpha_{pl}/\cos(\theta)$ where α_{pl} is the absorption for a planar surface and θ is the refracted angle [6]. The effect of the increased optical path-length in textured cells was simulated in PC1D for 45 Ω/sq and 100 Ω/sq cells. Figure 4 shows that the short-wavelength IQE was almost identical for the 100 Ω/sq textured and planar cells when other device parameters (i.e. FSRV) were unchanged. Similarly, the short-wavelength IQE results were almost identical for the simulated cells with 45 Ω/sq planar and textured emitter with the same FSRV. Therefore, the difference in the light path-length in a textured emitter versus a planar emitter has a negligible effect on the improvement due to the high sheet-resistance emitter.

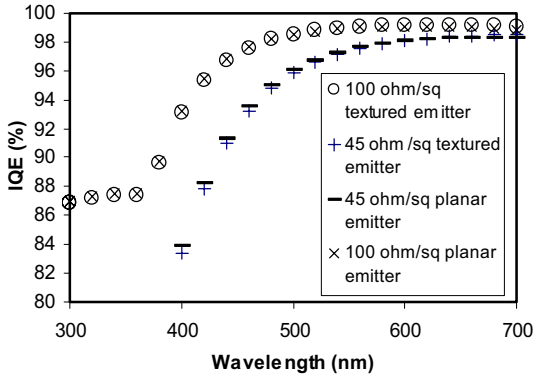

Fig. 4: PC1D-simulated short-wavelength response for textured and planar 100 and 45 Ω/sq emitter cells. FSRV is the same for all cases.

The second effect resulting in the higher ΔJ_{sc} and higher $\Delta\eta$ is due to the lower reflectance of the textured surface, which would result in a greater enhancement due to the high-sheet resistance emitter as compared to the enhancement for a planar emitter with the same passivation. This can be described by the following simple equation: $\Delta SR(\lambda)=\Delta IQE(\lambda)(1-R(\lambda))\cdot(\lambda/1.24)$, where ΔSR is the enhancement in spectral response due to ΔIQE. Therefore, for a lower reflectance the enhancement in spectral response due the high sheet-resistance emitter would be more pronounced. For the reflectance values obtained from Fig. 2, ΔJ_{sc} for the textured emitter would be more pronounced by a factor of 1.096 compared to the planar emitter. However, this factor does not account for more than ~0.1 mA/cm^2 of the improvement in ΔJ_{sc} in favor of the textured cells. This is also in agreement with PC1D modeling results assuming that the FSRV is the same for textured and planar cells for the same emitter (i.e. $\Delta IQE_{tex}\sim\Delta IQE_{pl}$).

The third aspect investigated is the FSRV difference between textured and planar cells for 100 and 45 Ω/sq emitters. This was found to be the main effect that results

in the greater performance enhancement observed due to the high sheet-resistance emitter for textured cells. This is because the change in FSRV between the 100 and 45 Ω/sq emitter is greater for textured than for planar cells. In order to prove this behavior the FSRV was extracted by matching the measured short-wavelength IQE with the PC1D-modeled IQE for planar and textured cells. As an example of the FSRV extraction, the measured and simulated short-wavelength IQE for a FZ cell with a 100 Ω/sq textured emitter is shown in Fig. 5. The extracted FSRV values for each case are shown in Table 2. The textured surface results in an area 1.73 times greater than that of the planar surface. The extracted FSRV values are in agreement with this area factor as shown in Table 2, where the FSRV for the textured emitter is ~1.7 times greater than that of the planar emitter, for the same emitter sheet-resistance. This is observed for both 45 and 100 Ω/sq emitters. As shown in Table 2, the effect of the FSRV change is more pronounced for the textured versus planar emitters resulting in a greater change in FSRV when going from the 45 Ω/sq emitter to the 100 Ω/sq emitter. This is because the effect of FSRV increase due to the textured area factor has less of an impact for the 100 Ω/sq emitter

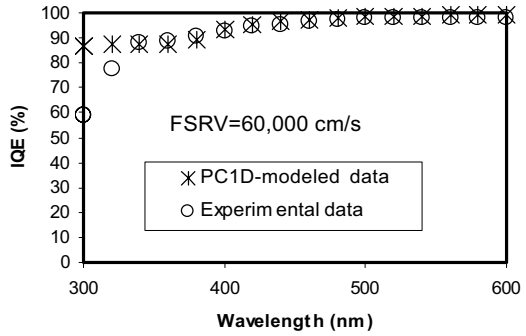

Fig. 5: IQE matching of experimental short-wavelength response data using PC1D-modeled data for 100 Ω/sq emitter textured cell.

with lower FSRV (35,000 cm/s for the planar emitter increases to 60,000 cm/s for the textured emitter) compared with the 45 Ω/sq emitter with a significantly higher FSRV (90,000 cm/s for the planar emitter increases to 150,000 cm/s for the textured emitter). Consequently, this more pronounced effect is reflected in the greater efficiency enhancement ($\Delta\eta$) for textured cells as shown in Fig. 3. The effect of the FSRV change for textured versus planar emitters is the main factor that results in the greater enhancement in ΔJsc of ~0.3 mA/cm^2 and $\Delta\eta$ of ~0.3% absolute in favor of textured cells. Using the FSRV values in Table 2, PC1D simulation results show an enhancement of ~0.4 mA/cm^2 in ΔJsc and 0.4% absolute in $\Delta\eta$ in favor of textured cells

Table 2: Extracted FSRV values for 45 and 100 Ω/sq textured and planar emitters.

Emitter ρ_s (Ω/sq)	Textured/Planar	FSRV (cm/s)	FSRV Factor Due to Textured Surface
45	planar	90,000	1.67
45	textured	150,000	
100	planar	35,000	1.71
100	textured	60,000	

for a 0.6 Ω-cm base resistivity, which supports the experimental results in Fig. 3.

B. Contact Interface Study

We have also investigated the contact interface for both textured and planar high sheet-resistance emitter cells. Figure 6 shows top-view SEM images of the area underneath the Ag gridline (25×25 μm) after etching away the bulk metal of the gridline and the glass layer. As shown in Fig. 6(a) the planar surface has a more irregular distribution of Ag segregation (or Ag crystallite precipitation) compared with the textured emitter surface in Fig. 6(b). Figure 6(b) shows that there is Ag precipitation at the peaks of the texture pyramids even in regions where the Ag crystallite precipitation is sparse. However, this is not the case for the planar surface where many regions are void of Ag crystallite precipitation. This results in a less regular distribution of Ag crystallites for the planar emitter surface as opposed to the textured emitter surface. This may explain the smaller standard deviation of 0.48 Ω-cm^2 in the series resistance for textured emitter cells compared with a standard deviation of 1.19 Ω-cm^2 for planar emitter cells. This may be attributed to the ease with which the glass frit can etch through the SiN_x layer for a textured surface, particularly at the peaks of the pyramids, compared with a planar emitter surface. However, more work is needed to support this result and to prove that it is not a surface orientation effect (i.e. (111) for a textured surface versus (100) for a planar surface). The fill factors achieved on the high-performance textured and planar 100 Ω/sq cells are very close comparing the high efficiency cells.

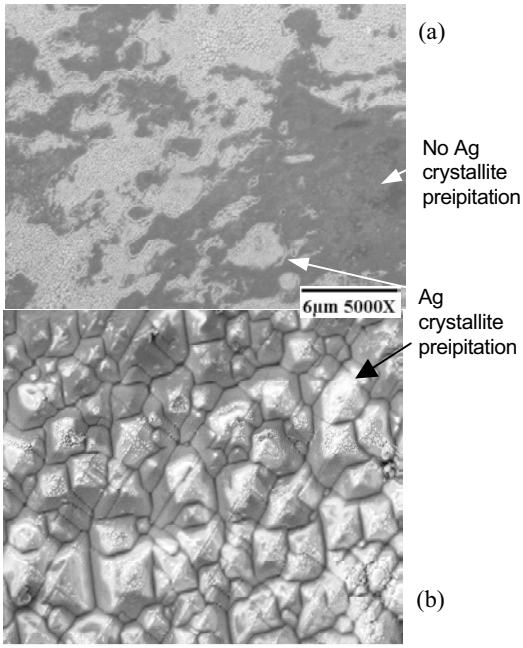

Fig 6: SEM top-view images of the region underneath the screen-printed contact for (a) planar emitter, and (b) textured emitter.

C. Record High-Efficiency Cell and Device Modeling

Through the understanding and implementation of

the above effects, we have fabricated record high-efficiency screen-printed cells of 18.8% with a textured 100 Ω/sq emitter (independently confirmed by NREL using a mask aperture area of 3.802 cm^2). This cell has 0.6 Ω-cm base resistivity and a single-layer antireflection coating (PECVD SiN_x), the original cell area is 4 cm^2. This high-efficiency is primarily due to the high current of 37.3 mA/cm^2 and high FF of 0.784 (Fig. 7) while maintaining a good V_{oc}. This high FF is made possible by the low series resistance of 0.79 Ω-cm^2 as well as the low J_{o2} value of ~18 nA/cm^2, which shows that the p-n-junction was not badly affected by the paste firing even at the peaks of the pyramid texture. The V_{oc} is also maintained to a reasonably good value of 641.5 mV for the textured SP 100 Ω/sq emitter cell. This V_{oc} is close to the V_{oc} of the planar 100 Ω/sq cell of ~646 mV, which indicates the small loss in V_{oc} due to the change in FSRV from 35,000 cm/s to 60,000 cm/s due to texturing (Table 2). Ten cells were confirmed by NREL with efficiencies in the range of 18.4% to 18.9% on 0.6 Ω-cm as well as 1.3 Ω-cm with both sides textured.

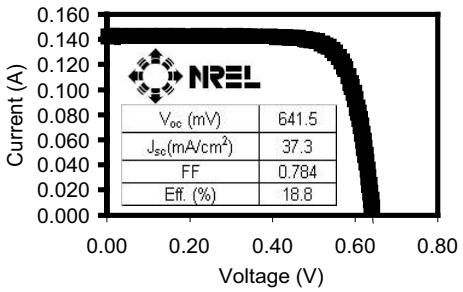

Fig. 7: I-V measurement by NREL for the 18.8% textured front and back 100-Ω/sq emitter cell.

Table 3 shows the PC1D device modeling parameters for an 18.6% 100 Ω/sq textured cell (also confirmed by NREL). The modeled parameters are obtained by matching the short- and long-wavelength IQE response while using the measured reflectance of the cell. The variation in the second-diode ideality factor (n_2) is probably responsible for the observed cell efficiency variation of 0.4% absolute for several high-efficiency cells fabricated in the same way. In agreement with the findings of Weeber et al. [7], our device modeling indicates that a better front-surface passivation (<20,000 cm/s) is necessary for further improvement of the 100 Ω/sq textured FZ cell to reach >20% cell efficiency.

Table 3: PC1D parameters that model the high efficiency 100 Ω/sq textured FZ cells.

Cell Parameters	Tex. 100 Ω/sq FZ
τ_{bulk}(μs)	250
BSRV (cm/s)	600
R_{back}(%)	61.5
FSRV (cm/s)	60,000
J_{o2}(nA/cm^2)	18
modelled V_{oc} (mV)	639
modelled J_{sc}(mA/cm^2)	37.1
modelled FF	0.785
modelled η (%)	18.6

CONCLUSION

Our results show synergism between high sheet-resistance emitter and a textured front-surface, which results in a greater efficiency enhancement due to the lightly doped textured emitter versus the enhancement due to the lightly doped emitter for planar cells. This is mainly attributed to the greater increase in FSRV due to texturing of the heavily doped emitters. The textured surface also shows more robustness in achieving consistently low series resistance compared with the planar emitter surface due to the ease of the Ag crystallite precipitation and contact formation at the tips of the texture pyramids. This work resulted in a high FF of 0.784 on 100 Ω/sq textured emitter and a record efficiency of 18.8% using a high-throughput SP contact co-firing process.

ACKNOWLEDGMENTS

This work was supported by NREL contract No. AAT-2-31605-02. The authors would like to thank Bobby To and Tom Moriarty at NREL for performing SEM and IV measurements, respectively.

REFERENCES

[1] J. Szlufcik, F. Duerinckx, E. Van Kerschaver, and J. Nijs, "Advanced Industrial Technologies for Multicrystalline Silicon Solar Cells," *17th EU PVSEC*, 2001, pp. 1271-1276.

[2] K. A. Münzer, K. H. Eisenthrith, R. E. Schlosser, and M. G. Winstel, "18%-PEBSCO-Silicon Solar Cells for Manufacturing," *17th EU PVSEC*, 2001, pp. 1363-1366.

[3] J. Nijs, E. Demesmaeker, J. Szlufcik, J. Poortmans, L. Frisson, K. De Clerq, M. Ghannam, R. Mertens, and R. Van Overstraeten, "Latest Efficiency Results with the Screen-printing Technology and Comparison with the Buried-Contact Structure," *1st WCPEC*, 1994, pp. 1242-1249.

[4] C. Schmiga, J. Schmidt, A. Metz, A. Endrös, and R. Hezel, "17.6% Efficient Tricrystalline Silicon Solar Cells with Spatially Uniform Texture," *Prog. Photovolt: Res. Appl.,* **11**, 2003, pp. 33-38.

[5] M. M. Hilali, A. Rohatgi and S. Asher, "Development of Screen-Printed Silcon Solar Cells with High Fill Factors on 100 Ω/sq Emitters," *IEEE Trans. on Elect. Dev.*, **51**, no. 6, 2004, pp. 948-955.

[6] P. A. Basore, "Extended Spectral Analysis of Internal Quantum Efficiency," *23rd IEEE PVSC*, 1993, pp.147-152.

[7] A. W. Weeber, A. R. Burgers, M. J. A. A. Goris, M. Koppes, E. J. Koppen, H. C. Rieffe, W. J. Soppe, C. J. J. Tool, and J. H. Bultman, "16% mc-Si Cell Efficiencies Using Industrial In-line Processing," *19th EU PVSEC*, 2004, in press.